

Morphological control of hybrid polymer-quantum dot solar cells with electron acceptor ligands

Mathieu Boivin, Sébastien Lamarre, Jonathan Tessier, Marie-Ève Lecavalier, Ahmed Najari et al.

Citation: *Appl. Phys. Lett.* **100**, 033302 (2012); doi: 10.1063/1.3678603

View online: <http://dx.doi.org/10.1063/1.3678603>

View Table of Contents: <http://apl.aip.org/resource/1/APPLAB/v100/i3>

Published by the [American Institute of Physics](http://www.aip.org).

Related Articles

Reevaluation of the beneficial effect of Cu(In,Ga)Se₂ grain boundaries using Kelvin probe force microscopy
Appl. Phys. Lett. **100**, 203903 (2012)

Direct and charge transfer state mediated photogeneration in polymer–fullerene bulk heterojunction solar cells
Appl. Phys. Lett. **100**, 193302 (2012)

Direct and charge transfer state mediated photogeneration in polymer–fullerene bulk heterojunction solar cells
APL: Org. Electron. Photonics **5**, 106 (2012)

Flexible thin-film InAs/GaAs quantum dot solar cells
Appl. Phys. Lett. **100**, 192102 (2012)

Two-photon excitation in an intermediate band solar cell structure
Appl. Phys. Lett. **100**, 172111 (2012)

Additional information on *Appl. Phys. Lett.*

Journal Homepage: <http://apl.aip.org/>

Journal Information: http://apl.aip.org/about/about_the_journal

Top downloads: http://apl.aip.org/features/most_downloaded

Information for Authors: <http://apl.aip.org/authors>

ADVERTISEMENT



Goodfellow
metals • ceramics • polymers • composites
70,000 products
450 different materials
small quantities fast

www.goodfellowusa.com

Morphological control of hybrid polymer-quantum dot solar cells with electron acceptor ligands

Mathieu Boivin,^{1,a)} Sébastien Lamarre,¹ Jonathan Tessier,¹ Marie-Ève Lecavalier,¹ Ahmed Najari,² Sophie Dufour-Beauséjour,¹ Evelynne Brown Dussault,¹ Pierre Collin,¹ and Claudine Ni. Allen^{1,b)}

¹Centre d'optique, photonique et laser (COPL), Département de physique, de génie physique et d'optique, Université Laval, 2375 rue de la Terrasse, Québec, G1V 0A6, Canada

²Département de chimie, Université Laval, 1045 avenue de la Médecine, Québec, G1V 0A6, Canada

(Received 3 October 2011; accepted 4 January 2012; published online 20 January 2012)

We integrate the electro-attractive conjugated molecule tetrafluoro-tetracyano-quinodimethane (F₄TCNQ) in the active layer of polymer-CdSe colloidal quantum dot (cQD) solar cells. The addition of this molecule enhances cQD dispersion inside the polymer. In tuning its concentration, we can optimize the active layer morphology for charge separation and transport. A smoother morphology is likely the result of polymer chain adsorption on cQDs via F₄TCNQ which increases the steric barrier between cQDs. Our most optimized device has a F₄TCNQ:cQDs weight ratio of 0.5% improving the power conversion efficiency by a factor ~ 2.3 . © 2012 American Institute of Physics. [doi:10.1063/1.3678603]

Hybrid organic-inorganic solar cells are promising devices for converting solar power into electricity at low fabrication costs. Bulk-heterojunction devices can be fabricated from blends of a semiconductive polymer as electron donor and semiconductor nanocrystals (NCs), as electron acceptors.¹⁻⁹ These solar cells aim to combine the qualities of organic and inorganic materials, i.e., easy processability and efficient charge transport. In addition to a good electron mobility, NCs have a wide absorption band tunable with their size and composition to fit the solar spectrum, and they are available in different shapes. The best power conversion efficiencies (PCEs) achieved with devices based on poly(3-hexylthiophene) (P3HT) as electron donor and CdSe NCs, such as nanorods, tetrapods, or hyperbranched, as electron acceptors are, respectively, 2.6%,⁵ 2.8%,⁶ and 2.2%.⁷ These elongated NC shapes provide more direct pathways for the charges to reach their electrodes.

However, other factors influence the hybrid solar cell performance. Indeed, the quality of the NC dispersion in the polymer film is an important issue in order to improve the device PCE. The NCs must be optimally dispersed in the polymer to constitute an interpenetrating network in order to obtain efficient exciton separation and charge transport in the active layer.^{4,11} Modification of the NC surface chemistry by ligand exchange is the most commonly used method to control NC dispersion in semiconductive polymers.²⁻¹¹ The initial ligands are usually exchanged for shorter ones, such as pyridine, to promote polymer-NC charge transfer by reduction of the potential barrier between the two materials and to improve NC-NC charge transport by phase segregation of NC domains. To control aggregation during film formation, additional ligands can be incorporated in the active layer mixture to increase NC solubility.^{4,11} However, conjugated polymers are usually insoluble in these ligands, so the added ligand concentration must be carefully adjusted to obtain a proper dispersion of both materials.

In this work, we integrate the electro-attractive conjugated molecule tetrafluoro-tetracyano-quinodimethane (F₄TCNQ) with P3HT and CdSe colloidal quantum dots (cQDs) in the active layer of hybrid solar cells. The addition of F₄TCNQ in the system makes it possible to control the surface roughness of the active layer without compromising on P3HT solubility in its original solution. F₄TCNQ has also been shown to form charge transfer complexes with both P3HT (Ref. 12) and bulk CdSe,¹³ possibly affecting the potential barrier between them.

Solar cell fabrication begins by preparing CdSe cQDs with a diameter around 4 nm whose synthesis methods are described elsewhere.¹⁴ Synthetic ligands on cQDs are replaced by refluxing them in pyridine for 24 h. After this treatment, the cQDs are precipitated in hexanes and rinsed twice to remove excess pyridine followed by redispersion in 1,2-dichlorobenzene (DCB). Also, F₄TCNQ and P3HT are co-dissolved in various weight ratios in DCB. These two solutions are mixed together to obtain a P3HT:cQDs weight ratio of 1:8 with a P3HT concentration of 6.6 mg/mL in the final blend. This blend is then heated at a temperature around 70 °C before a 1.0- μ m filtering followed by spin-coating to form the active layer on an ITO substrate covered by a poly(3,4-ethylenedioxythiophene):poly(styrenesulfonate) hole transport layer. The active layer thickness is typically between 70 and 120 nm. The device is then annealed at 120 °C during 15 min under nitrogen atmosphere. Finally, a 70 nm thick aluminum cathode is deposited by thermal evaporation, yielding an active area of 0.25 cm². Active layer surface topography images were measured with a Veeco Dimension V atomic force microscope (AFM) and attenuated total reflectance Fourier transform infrared spectra (ATR-FTIR) were acquired by a Nicolet Magna IR 760 spectrometer equipped with a Golden Gate ATR system. All fabrication and characterization steps, except device annealing and cathode deposition, were carried out in ambient air.

The current density-voltage (J-V) curves of our best solar cells with and without F₄TCNQ under AM1.5G illumination are shown in Fig. 1(a). The irradiance of (400 \pm 50) mW/cm²

^{a)}Electronic mail: mathieu.boivin.4@ulaval.ca.

^{b)}Electronic mail: claudine.allen@phy.ulaval.ca.

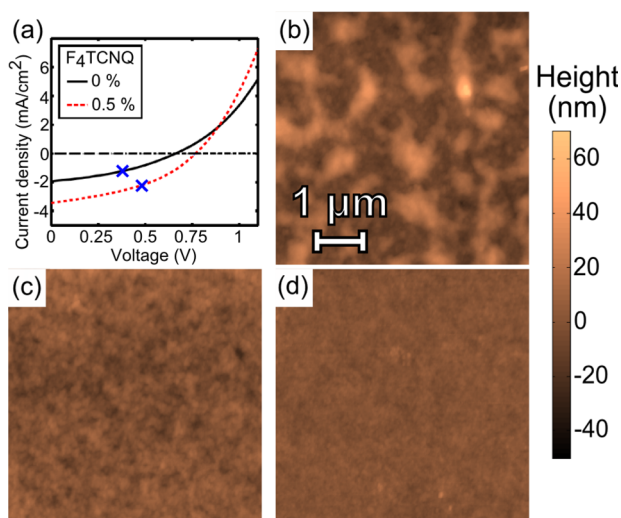


FIG. 1. (Color online) (a) Current density-voltage (J-V) curves of P3HT-cQD solar cells without (black line) and with F₄TCNQ (red dashed line) under AM1.5G illumination. The blue markers indicate the operating points with the highest PCE. AFM images of active layers having F₄TCNQ:cQDs weight ratios of (b) 0%, (c) 0.63%, and (d) 1.25%.

could not be measured very precisely, but the source was quite stable with less than 2% intensity fluctuations, hence enabling accurate relative PCE measures to demonstrate the effect of adding F₄TCNQ. The device with a F₄TCNQ:cQDs weight ratio of 0.5% exhibited an open-circuit voltage (V_{oc}) of 0.76 V and a short-circuit current density (J_{sc}) of 3.44 mA/cm², leading to a fill factor (FF) of 0.41. Comparing to the device without F₄TCNQ, its characteristics were a V_{oc} of 0.66 V, a J_{sc} of 1.95 mA/cm² and a FF of 0.36. We also noted that the external quantum efficiency usually peaked around 500 nm. In this case, the addition of F₄TCNQ leads to an increase in PCE of ~2.3 times, which is attributed to an improved active layer morphology.

Figures 1(b)–1(d) present AFM images for three films made from solutions having different F₄TCNQ:cQDs weight ratios. The surface of the active layer becomes smoother with smaller aggregates as the amount of incorporated F₄TCNQ is increased. This observation could be explained by a better cQD dispersion in the P3HT film due to the presence of F₄TCNQ. More quantitatively in Fig. 2, the root mean square (RMS) surface roughness for different active layers was calculated from AFM topography images as a function of the F₄TCNQ:cQDs weight ratio from 0% to 1.2% and we observed a diminution in the mean RMS value by a factor of ~5.7. The red box plot also in Fig. 2 represents the PCE normalized by the average value without F₄TCNQ. When the solar cells have a F₄TCNQ:cQDs weight ratio between 0.38% and 0.63%, their PCE is distributed on higher values. At these weight ratios, the mean RMS surface roughness is generally less than 10 nm, thus we assume that the cQD dispersion in the active layer creates optimal structures for efficient exciton separation and charge transport to the electrodes. When the F₄TCNQ:cQDs weight ratio is 1.2%, the PCE distribution drops back to lower values comparable to those of the solar cells containing no F₄TCNQ. The cause of this reduction is most likely the cQD dispersion becoming too scattered inside the active layer, hence hindering charge transport by introducing discontinuities in the percolation

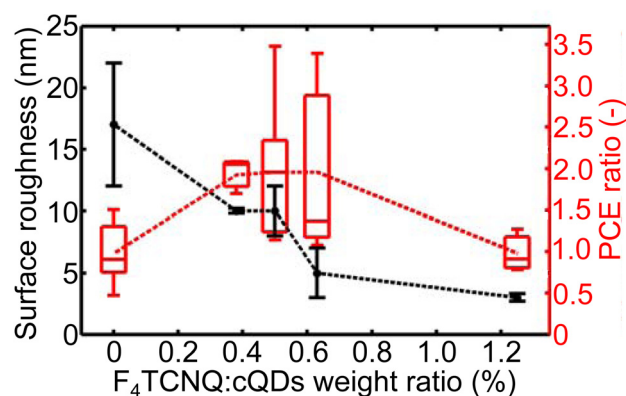


FIG. 2. (Color online) The mean surface roughness (black dots) and the box plot of PCE distributions (red) are shown for different F₄TCNQ concentrations, with the later ratio relative to the 0% F₄TCNQ leftmost data. The distributions were obtained from 14, 3, 5, 7, and 5 solar cells for each dataset respectively from left to right, with black error bars giving the standard deviation of the surface roughness while the red dashed line goes through the mean PCE value. For each distribution, the mean J_{sc} is 2.0 ± 0.9 mA/cm², 3.0 ± 0.3 mA/cm², 2.2 ± 0.7 mA/cm², 2.7 ± 1.4 mA/cm², and 1.6 ± 0.3 mA/cm², respectively.

pathways. The relatively wide extent of the PCE distributions is attributed to variations in the fabrication process of the bulk-heterojunction solar cells. These variations can dramatically affect device performance.^{15,16} Some examples are small changes in material blend ratios,^{17,18} reproducibility of the ligand exchange,^{11,19} and variations of the average active layer thickness.¹⁸

To understand how the addition of F₄TCNQ modifies the morphology of P3HT-cQD solar cells, we measured the ATR-FTIR spectra of four samples: (1) F₄TCNQ, (2) cQD-F₄TCNQ, (3) P3HT-F₄TCNQ, and (4) P3HT-cQD-F₄TCNQ (Fig. 3(a)). Sample 1 was a powder while samples 2, 3, and 4 were cast in solid film for this experiment. The second and third samples had F₄TCNQ:cQDs and F₄TCNQ:P3HT weight ratios of 2.1% and 8.6%, respectively. The last P3HT-cQD-F₄TCNQ blend was prepared like samples 2 and 3 while keeping a 1:4 P3HT:cQDs weight ratio. We focused our analysis on the absorption of the cyano bond C \equiv N, which is a sensitive charge indicator on the F₄TCNQ molecule.¹² Its spectral signature highlights the formation of charge-transfer (CT) complexes involving F₄TCNQ. For neutral F₄TCNQ in

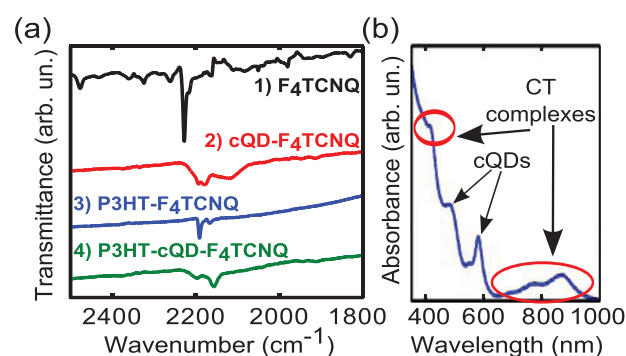


FIG. 3. (Color online) (a) ATR-FTIR spectra of (1) F₄TCNQ powder, (2) cQD-F₄TCNQ solid film, (3) P3HT-F₄TCNQ solid film, and (4) P3HT-cQD-F₄TCNQ solid film. (b) Absorption spectrum of the cQD-F₄TCNQ blend (sample 2) in a dichlorobenzene solution.

powder, the $C \equiv N$ absorption peak is sharp and centered at 2227 cm^{-1} . When $F_4\text{TCNQ}$ is mixed with P3HT and/or cQDs in the last three samples, the $C \equiv N$ peak is red-shifted, broadened, and even split into a few peaks. This is characteristic of the $F_4\text{TCNQ}$ anion radical state due to the formation of CT complexes. Interestingly, these CT complexes also introduce absorption bands in the cQD visible spectrum as shown by the red circles in Fig. 3(b). The more crucial point of this analysis is that for the P3HT-cQD- $F_4\text{TCNQ}$ blend (Fig. 3(a), sample 4), the $C \equiv N$ absorption does not have the same spectral signature as samples 2 and 3 where the $F_4\text{TCNQ}$ is interacting separately with the cQDs and the P3HT. These measurements demonstrate that a new kind of CT complex occurs in the P3HT-cQD- $F_4\text{TCNQ}$ film where the three compounds are interacting together. Thus, our hypothesis to explain the decreasing roughness of our polymer-cQD solar cells is the adsorption of P3HT chains on cQDs through $F_4\text{TCNQ}$ molecules binding both the polymer and the cQD surface. This adsorption increases the steric barrier between the cQDs, enhancing their dispersion inside the active layer to give more polymer-cQD interface for charge separation.

In conclusion, the incorporation of $F_4\text{TCNQ}$ in the active layer of P3HT-CdSe cQD solar cells makes it possible to optimize its morphology by decreasing its RMS surface roughness. We assume that $F_4\text{TCNQ}$ molecules complexing the cQD surface also form CT complexes with surrounding P3HT polymer chains, hence increasing the steric barrier between the cQDs and enhancing their dispersion inside the active layer. Our most optimized device has a $F_4\text{TCNQ}$:cQDs weight ratio of 0.5% yielding a PCE ~ 2.3 times higher than our best solar cell without $F_4\text{TCNQ}$.

We acknowledge financial support from the Natural Sciences and Engineering Research Council of Canada (NSERC) and we thank Souleymane Toubou Bah, Patrick Larochelle, Dr. Simon Frédérick, and Alexandre Aquin for technical support and fruitful scientific discussions.

- ¹N. C. Greenham, X. Peng, and A. P. Alivisatos, *Phys. Rev. B* **54**, 17628 (1996).
- ²D. S. Ginger and N. C. Greenham, *J. Appl. Phys.* **87**, 1361 (2000).
- ³W. Huynh, J. J. Dittmer, and A. P. Alivisatos, *Science* **295**, 2425 (2002).
- ⁴W. Huynh, J. J. Dittmer, W. Libby, G. Whiting, and A. P. Alivisatos, *Adv. Funct. Mater.* **13**, 73 (2003).
- ⁵B. Sun and N. C. Greenham, *Phys. Chem. Chem. Phys.* **8**, 3557 (2006).
- ⁶B. Sun, H. J. Snaith, A. S. Dhoot, S. Westenhoff, and N. C. Greenham, *J. Appl. Phys.* **97**, 014914 (2005).
- ⁷I. Gur, N. A. Fromer, C. Chen, A. G. Kanaras, and A. P. Alivisatos, *Nano Lett.* **7**, 409 (2007).
- ⁸S. Kumar and G. D. Scholes, *Microchim. Acta* **160**, 315 (2007).
- ⁹B. R. Saunders and M. L. Turner, *Adv. Colloid. Interface Sci.* **138**, 1 (2008).
- ¹⁰D. Aldakov, F. Chandezon, R. D. Bettignies, M. Firon, P. Reiss, and A. Pron, *Eur. Phys. J.: Appl. Phys.* **36**, 5 (2006).
- ¹¹J. Olson, G. Gray, and S. Carter, *Sol. Energy Mater. Sol. Cells* **93**, 519 (2009).
- ¹²K. Yim, G. L. Whiting, C. E. Murphy, J. J. M. Halls, J. H. Burroughes, R. H. Friend, and J. Kim, *Adv. Mater.* **20**, 3319 (2008).
- ¹³J. Z. Zhang and A. B. Ellis, *J. Phys. Chem.* **96**, 2700 (1992).
- ¹⁴C. R. Bullen and P. Mulvaney, *Nano Lett.* **4**, 2303 (2004).
- ¹⁵B. T. de Villers, C. J. Tassone, S. H. Tolbert, and B. J. Schwartz, *J. Phys. Chem. C* **113**, 18978 (2009).
- ¹⁶H. Hoppe and N. S. Sariciftci, *J. Mater. Chem.* **16**, 45 (2006).
- ¹⁷M. Reyes-Reyes, K. Kim, and D. L. Carroll, *Appl. Phys. Lett.* **87**, 083506 (2005).
- ¹⁸A. J. Moulé, J. B. Bonekamp, and K. Meerholz, *J. Appl. Phys.* **100**, 094503 (2006).
- ¹⁹I. Lokteva, N. Radychev, F. Witt, H. Borchert, J. Parisi, and J. Kolny-Olesiak, *J. Phys. Chem. C* **114**, 12784 (2010).